Noise and entanglement in quantum conductors

G.B. Lesovik and A.V. Lebedev

L.D. Landau Institute for Theoretical Physics, RAS, 119334 Moscow, Russia
Theoretische Physik, Schafmattstrasse 32, ETH-Zurich, CH-8093, Zurich, Switzerland

Abstract. In this article we discuss our two recent proposals on producing and detecting of entangled states in quantum conductors. First we analyze a setup where two electrons are scattered on a quantum dot with Coulomb repulsion and became orbitally entangled. Second, for identical noninteracting particles we suggest an operating scheme for the deliberate generation of spin-entangled electron pairs in a normal-metal mesoscopic structure with a fork geometry. The spin-entangled pair is created through a post-selection in the two branches of the fork. We also make comments on different ways of producing and quantifying the degree of entanglement.

Keywords: entanglement, noise, electronic transport
PACS: 73.23.-b, 03.65.Nk, 03.67.Mn

INTRODUCTION

Quantum mechanics is a non-deterministic theory, where one can not predict results of all measurements with certainty. A simplest example is the tunneling of the electron through a barrier. After the scattering electron may tunnel through the barrier with a finite probability T or may be reflected back with probability $R = 1 - T$. In analogy with optics, this phenomena is known as partitioning of the wave function. This type of phenomena requires probabilistic description which turns out to be the only accessible way in general situation for quantum systems, as was first pointed out by Born [1].

The partitioning of the wave function reveals itself in the shot noise phenomenon in coherent conductors, where Fermi statistics suppress fluctuations in the number of particles incoming from reservoir [2]. The shot noise can be observed by measuring the second order current-current correlators that requires a very elaborate experiment in practice [3]. In general, noise measurements provide more information about the system then the measurement of conductance alone. As an example, measurement of the shot noise allows one to probe the charge of the carriers [4]. Going beyond the second order correlators, one could study the full counting statistics (FCS) that is the probability to transmit n electrons through a barrier during a given time interval [5]. To measure FCS, one needs even more elaborate setup, which has been realized for electrons [6]. Still the experimental setup for measuring FCS were electrons flying ballistically remains to be challenging.

A more complicated type of uncertainty in quantum mechanics appears in the joint state of two systems A and B which have been interacted in the past. Then the outcome of the measurement on the system A will in general depend on a state of the system B even if two systems are spatially separated and no longer interact with each other. The appearance of such correlations between two systems is not a surprise even in the classical physics. What is amazing is that these correlation in the quantum case, as was first shown by Bell [7], may be stronger than any possible classical correlations adopting the Einstein locality principle.

The situation where the state of the system B correlated with the system A is unknown can be described by the density matrix ρ_A introduced independently by Landau [8] and von Neumann [9]. In this case the state of the system A is mixed, i.e. can not be described by the wave function as it can be done for pure states. To distinguish between pure and mixed states one could calculate the purity $\Pi_A = \mathrm{tr}\{\rho_A^2\}$ which equals to 1 for pure states and $\Pi_A < 1$ for the mixed ones [10].

For a long time this type of correlation was mostly considered as the source of the decoherence of the system A by some reservoir B, spoiling the quantum behaviour of the system A. Nowadays it is very well understood that such mixed states with $\Pi_A < 1$ describe an entangled state of two systems A and B, a concept first introduced by Einstein Podolsky and Rosen [11] and Schroedinger [12]. Provided the full control on the state of the system B, today these quantum correlations between entangled systems are regarded as a resource for various sort of the quantum information schemes like cryptography and quantum computation. In addition, one may study fundamental aspects of the quantum theory like locality in quantum mechanics by measuring proper correlations between the systems A and B, checking e.g. Bell inequality [7, 13].

Various setups were proposed for producing isolated entangled particles and detecting the presence of the entanglement by testing the Bell inequality via measuring cross correlators for the currents [14, 15], see Ref. [16]

for a recent review. As we have already noted, to check the entanglement presence one may use purity or von Neumann entropy. Nevertheless it is not always clear what would be the experimental procedure to check all components of the density matrix. Moreover, in general $\Pi_A < 1$ does not guarantee that the system A is not entangled with some other system C e.g. with an uncontrolled environment. Testing the Bell inequality via measuring proper correlation between particles remains to be the most reliable way to detect the entanglement. Although such an experiment was successfully realized in optics [17], the corresponding experiment for the massive particles remains to be challenging. To make some progress, one could measure instead more accessible quantities of the total system $A+B$ e.g. magnetization which may indicate the presence of entanglement [18]. In this case, one has to strongly rely on a particular theoretical model, describing the system.

In this article we discuss our two recent proposals on producing and detecting of entangled states in quantum conductors. The generic way for two particles become entangled is to let them interact with each other. In [19] we analyzed a setup where two electrons are scattered on a quantum dot with Coulomb repulsion. Characterizing the dot by its resonances we have derived an exact formula for the N particle scattering matrix. We make use of our results to study the interaction-induced orbital entanglement of two electrons incident on the dot in a spin-singlet state.

For the identical particles one can create an entangled state by a post-selection of measured outcomes without direct interaction [20]. In [15] we suggest an operating scheme for the deliberate generation of spin-entangled electron pairs in a normal-metal mesoscopic structure with a fork geometry. Voltage pulses with associated Faraday flux equal to one flux unit $\Phi = hc/e$ drive individual singlet-pairs of electrons towards the beam splitter. The spin-entangled pair is created through a post-selection in the two branches of the fork. We analyze the appearance of entanglement in a Bell inequality test formulated in terms of the number of transmitted electrons with a given spin polarization.

ENTANGLEMENT DUE TO COULOMB INTERACTION

In this section we follow our recent paper [19], where we derived the N-particle scattering matrix for electrons propagating through quantum dot with Coulomb repulsion. The scattering matrix, taking asymptotically free incoming states through an interaction region and providing the free outgoing states, is of huge basic and practical interest. Originally introduced by Born [1] and by Wheeler and independently by Heisenberg [21] in atomic and particle physics, its application to electron transport [22] has made it into a central tool of mesoscopic physics. Its formulation for non-interacting electrons provides the two-terminal conductance [22], non-equilibrium noise [2] and the full counting statistics [5] in terms of the transmission probability across the scatterer. In interacting case the scattering matrix besides the transport characteristics allows one to study degree of entanglement of a many-particle scattered state induced by interaction. The entanglement between electrons can be studied in a new type of transport experiment, where specially designed electron sources send a finite number of electrons towards the scattering region [23, 24], see Ref. [25] for recent experiments in this direction.

Within our formalism, the interaction is accounted for by the Hamiltonian $\hat{H}_{\rm int} = e^2\hat{N}^2/2C$, where $\hat{N}$ is the dot's electron number operator and C denotes its capacitance. We use two-particle scattering matrix to study the wave function and degree of entanglement of two scattered electrons. Below, we construct the two-particle scattering matrix for the quantum dot including Coulomb interaction and generalize the result to the N-particle situation. For a quantum dot with a single resonance our model is equivalent to the Anderson impurity model [26] up to the self-interaction energy $e^2\hat{N}/2C$, which leads to the renormalization of the bare resonance energy $\varepsilon \to \varepsilon + e^2/2C$, see below.

Usually, the scattering matrix connects states at given energies; here, we start with the propagator describing the scattering of wave packets in coordinate space. We start with a (properly symmetrized, spin indices are suppressed) incident two-electron wave function at time t_1, $\Psi^{\rm in}(\vec{y},t_1)$, with $\vec{y} = \{y_1, y_2\}$. The scattered wave function at later times $t_2 > t_1$ can be obtained with the help of the two-particle propagator $K^{(2)}(\vec{x},t_2;\vec{y},t_1)$ describing the evolution of two particles from the initial positions $\vec{y}$ at time t_1 to the final positions $\vec{x}$ at t_2,

$$\Psi^{\rm out}(\vec{x},t_2) = \int d^2y\, K^{(2)}(\vec{x},t_2;\vec{y},t_1)\,\Psi^{\rm in}(\vec{y},t_1). \quad (1)$$

The two-particle propagator $K^{(2)}$ can be defined through a Feynman path integral over trajectories $\vec{x}(t)$,

$$K^{(2)}(\vec{x},t_2;\vec{y},t_1) = \int \mathscr{D}[\vec{x}]\, \exp\Big(\frac{i}{\hbar}\int_{t_1}^{t_2} dt\, L^{(2)}(\vec{x};\dot{\vec{x}})\Big), \quad (2)$$

with the boundary conditions $\vec{x}(t_1) = \vec{y}$. Here, $L^{(2)}(\vec{x},\dot{\vec{x}})$ is the system's Lagrangian including kinetic ($\propto m$), dot potential (U), and interaction ($\propto U_c = 2e^2/C$) energies,

$$L^{(2)} = \sum_{i=1}^{2}\Big[\frac{m\dot{x}_i^2}{2} - U(x_i)\Big] - \frac{U_c}{4}\big[\chi_{\rm d}(x_1)+\chi_{\rm d}(x_2)\big]^2, \quad (3)$$

with the characteristic function $\chi_{\rm d}(x)$ of the dot equal to unity within the dot and zero outside.

Without interaction, the two-particle propagator factorizes, $K^{(2)}(\vec{x},t_2;\vec{y},t_1) = \Pi_i K^{(1)}(x_i,t_2;y_i,t_1)$ with $K^{(1)}(x,t_2;y,t_1)$ the one-particle propagator, while the interaction mixes the particle trajectories. A Hubbard-Stratonovich transformation with the real auxiliary field $z(t)$ allows us to decouple the quadratic interaction

$$K^{(2)}(\vec{x},t_2;\vec{y},t_1) = \int \mathscr{D}[z] \exp\Big[i\frac{U_c}{\hbar}\int dt\, z^2(t)\Big] \times K^{(1)}_{[z]}(x_1,t_2;y_1,t_1)\, K^{(1)}_{[z]}(x_2,t_2;y_2,t_1), \quad (4)$$

where $K^{(1)}_{[z]}(x,t_2;y,t_1)$ is the one-particle propagator in the presence of a fluctuating potential $U_c(t) = U_c z(t)$,

$$K^{(1)}_{[z]} = \int \mathscr{D}[x] \exp\Big[\frac{i}{\hbar}\int_{t_1}^{t_2} dt\,\Big(\frac{m\dot{x}^2}{2} - U(x) - U_c z(t)\chi_{\rm d}(x)\Big)\Big].$$

Next, we introduce the scattering matrix $S^{(1)}_{\alpha\beta}(\varepsilon) \equiv \mathbf{S}^{(1)}(\varepsilon)$ of the dot in the absence of the fluctuating potential $U_c(t)$; the indices $\alpha,\beta \in \{\text{L,R}\}$ specify the lead indices for the outgoing (α) and incoming (β) scattering channels. We describe the dot through the resonance positions (ε_j) and (identical) widths (Γ); the scattering matrix $S^{(1)}_{\alpha\beta}(\varepsilon)$ then takes the form

$$S^{(1)}_{\alpha\beta}(\varepsilon) = r_{\alpha\beta} + \sum_j \frac{i\Gamma/2}{\varepsilon - \varepsilon_j + i\Gamma/2}\, s^{(j)}_{\alpha\beta}, \quad (5)$$

where the constant 2×2 matrices $\mathbf{r}$ and $\mathbf{s}^{(j)}$ can be found from the unitarity conditions. The Fourier transform provides the real time (τ) representation

$$S^{(1)}_{\alpha\beta}(\tau) = \delta(\tau) r_{\alpha\beta} + \theta(\tau)\sum_j \frac{\eta}{2} e^{-i\omega_j\tau} e^{-\eta\tau/2} s^{(j)}_{\alpha\beta}, \quad (6)$$

where $\eta = \Gamma/\hbar$ is the inverse dwell time, $\omega_j = \varepsilon_j/\hbar$ is the resonance frequency, and $\delta(\tau)$, $\theta(\tau)$ are the usual δ- and Heaviside functions. The first term in Eq. (6) describes the reflection of a particle that has not penetrated into the dot, while the subsequent terms correspond to processes where the particle has spent a time τ inside the dot; the factor $e^{-i\omega_j\tau}$ describes the accumulated phase. The presence of the fluctuating potential $U_c(t)$ contributes an additional phase to the one-particle scattering matrix (6),

$$S^{(1)}_{\alpha\beta,[z]}(t_2,t_1) = S^{(1)}_{\alpha\beta}(t_2-t_1)\exp\Big(-\frac{i}{\hbar}\int_{t_1}^{t_2} U_c(t)dt\Big), \quad (7)$$

where t_1 and t_2 denote the arrival and escape times of the particle (we assume escape amplitudes that depend weakly on energy).

Next, we express the propagator $K^{(1)}_{[z]}$ through the scattering matrix (7). To simplify matters, we linearize the spectrum, $\varepsilon(k) = \hbar v k$; a particle escaped out of the dot then never returns. In terms of trajectories, the scattering process involves three stages: *i)* the ballistic motion with velocity v towards the dot, *ii)* the dwell time in the dot, and, *iii)* the ballistic propagation away from the dot. We define the coordinates in the left ($x<0$) and right ($x>0$) leads with respect to the left ($x=0^-$) and right ($x=0^+$) dot boundaries and express the propagator $K^{(1)}_{[z]}$ through the scattering matrix (7), $K^{(1)}_{\alpha\beta,[z]}(x,t_2;y,t_1) = S^{(1)}_{\alpha\beta,[z]}(\tau,s)/v$, where $s = t_1 + |y|/v$ and $\tau = t_2 - |x|/v$ are the arrival and escape times of the particle to and from the dot. Similar definitions ($s_i = t_1 + |y_i|/v$ and $\tau_i = t_2 - |x_i|/v$) apply to the two-particle scattering matrix: $\mathbf{S}^{(2)}_{[z]}(\tau_1,\tau_2;s_1,s_2) = S^{(1)}_{\alpha_1\beta_1,[z]}(\tau_1,s_1) S^{(1)}_{\alpha_2\beta_2,[z]}(\tau_2,s_2)$. Taking the average with respect to the fluctuating Gaussian field $z(t)$, $\langle z(t_2)z(t_1)\rangle = (i/2\omega_c)\delta(t_2-t_1)$, $\omega_c = U_c/\hbar$ one could arrive to the result

$$\mathbf{S}^{(2)}(\vec{\tau};\vec{s}) = \tilde{\mathbf{S}}^{(1)}(\tau_1 - s_1)\otimes\tilde{\mathbf{S}}^{(1)}(\tau_2 - s_2)\exp(-i\frac{\omega_c\tau_{12}}{2}), \quad (8)$$

where $\tilde{\mathbf{S}}^{(1)}$ is the scattering matrix (6) with renormalized resonance energies $\tilde{\varepsilon}_j = \varepsilon_j + U_c/4$ and τ_{12} is the time the two particles spend together in the dot,

$$\tau_{12} = \tfrac{1}{2}(|\tau_1 - s_2| + |\tau_2 - s_1| - |\tau_1 - \tau_2| - |s_1 - s_2|).$$

This two-particle scattering matrix (8) is the key result of this Section. All effects of Coulomb interaction are accounted for by renormalized resonance energies due to self-interaction of individual electrons in the dot and an additional phase accumulated by the electrons during their simultaneous presence in the quantum dot. The self-interaction of electrons may arise due to the screening environment in realistic quantum dots, while in the absence of the screening (e.g. in Anderson impurity model) one has to use the bare resonance energies ε_j in Eq. (8).

Below we concentrate on a single level quantum dot with no self-interaction present. An inverse Fourier transformation provides us with the energy representation

$$\mathbf{S}^{(2)}(\vec{\varepsilon}';\vec{\varepsilon}) = \delta_{\varepsilon_1\varepsilon_1'}\delta_{\varepsilon_2\varepsilon_2'}\,\mathbf{S}^{(1)}(\varepsilon_1)\otimes\mathbf{S}^{(1)}(\varepsilon_2) + 2\pi\delta(\varepsilon_1+\varepsilon_2-\varepsilon_1'-\varepsilon_2')\mathbf{S}_{U_c}(\vec{\varepsilon}';\vec{\varepsilon}), \quad (9)$$

where the second term accounts for inelastic processes where only the total energy $E = \varepsilon_1 + \varepsilon_2$ is conserved:

$$\mathbf{S}_{U_c}(\vec{\varepsilon}';\vec{\varepsilon}) = \frac{(iU_c/2)\,\mathbf{s}\otimes\mathbf{s}}{\varepsilon_1+\varepsilon_2-2\varepsilon_0-\frac{U_c}{2}+i\Gamma}\,\frac{i\frac{\Gamma}{2}}{\varepsilon_1-\varepsilon_0+i\frac{\Gamma}{2}} \times\frac{i\frac{\Gamma}{2}}{\varepsilon_2-\varepsilon_0+i\frac{\Gamma}{2}}\left(\frac{1}{\varepsilon_1'-\varepsilon_0+i\frac{\Gamma}{2}}+\frac{1}{\varepsilon_2'-\varepsilon_0+i\frac{\Gamma}{2}}\right). \quad (10)$$

The Coulomb interaction generates additional pole at $E = 2\varepsilon_0 + U_c/2 - i\Gamma$ of the total energy E. This interaction-induced singularity cannot be obtained via a perturbative expansion for large $U_c \gg \Gamma$.

The above derivation for the two-particle scattering matrix can be generalized to N particles, where appear an additional phase factors accounting for the pairwise interaction of particles residing simultaneously (for a time τ_{jk}) on the dot,

$$S^{(N)}_{\{\alpha_j\beta_j\}}\big(\{\tau_j;s_j\}\big)=\prod_{j>k}^{N}e^{-i\omega_c\tau_{jk}/2}\prod_{j=1}^{N}\tilde{S}^{(1)}_{\alpha_j\beta_j}(\tau_j-s_j).$$

The above result also holds true for a multichannel setup, with $\alpha_j,\ \beta_j,\ j=1,\ldots,N$ turning into multichannel indices. In particular, the results can be straightforwardly applied to the experimental setup [27] with two parallel leads feeding/emptying two capacitively coupled dots that has been recently used to measure interaction-induced cross correlations, see also Ref. [28].

In applying our results to realistic mesoscopic problems, we have to avoid mixing between the scattered particles and the electrons in the Fermi sea. Hence, we do not consider situations with levels within the distance Γ around the Fermi energy $\varepsilon_{\rm F}$ and assume that U_c does not shift a level across $\varepsilon_{\rm F}$; the latter allows us to ignore complications due to the Kondo effect [29]. In the following, we study the scattering problem of two single-electron excitations created above the Fermi sea and a quantum dot with only one resonance at ε_0 above the Fermi energy $\varepsilon_{\rm F}$, $\varepsilon_0-\varepsilon_{\rm F}\gg\Gamma$. The scattering matrix (10) then tells, that (the non-trivial component of) the scattered wave function involves energies near ε_0 and $\varepsilon_+=\varepsilon_0+U_c/2$.

We start from a two-electron state $\Psi^{\rm in}(x_1,x_2)$ disentangled with the Fermi sea created at time $t=0$ in the left lead and moving towards to the dot. This could be achieved either by applying a unit-flux voltage pulse of the Lorenzian form [23] or by using a specially designed single electron injector [24, 25]. The scattered wave is given by Eq. (1) and can be expressed in terms of retarded variables $\xi_{1,2}=|x_{1,2}|-v_{\rm F}t$, with $v_{\rm F}$ the Fermi velocity. The scattered wave to the right of the dot involving tunneling of both electrons assumes the form $\Psi(\xi_1,\xi_2)=\Psi_{sq}(\xi_1,\xi_2)+\Psi_{U_c}(\xi_1,\xi_2)$, with ($Y\equiv y_1+y_2$)

$$\Psi_{sq}=\frac{s_{\rm RL}^2}{\ell^2}\int_{\xi_<}^{\xi_>}dy_1\int_{\xi_>}^{0}dy_2\,e^{ik_0(\xi_1+\xi_2-Y)}e^{(\xi_1+\xi_2-Y)/\ell}$$
$$\times\big[\theta(\xi_2-\xi_1)\Psi^{\rm in}(y_1,y_2)+\theta(\xi_1-\xi_2)\Psi^{\rm in}(y_2,y_1)\big],$$

$$\Psi_{U_c}=\frac{s_{\rm RL}^2}{\ell^2}e^{ik_+\xi_>}e^{ik_0\xi_<}\int_{\xi_>}^{0}dy_1dy_2\,\Psi^{\rm in}(y_1,y_2)$$
$$\times e^{-ik_c(Y-|y_1-y_2|)/2}e^{-ik_0Y}e^{(\xi_1+\xi_2-Y)/\ell}\qquad(11)$$

where $\ell=2\hbar/\Gamma v_{\rm F}$ is the real-space width of the scattered wave, $\xi_>=\max\{\xi_1,\xi_2\}$, $\xi_<=\min\{\xi_1,\xi_2\}$, $k_0=\omega_0/v_{\rm F}$, $k_c=\omega_c/2v_{\rm F}$, and $k_+=k_0+k_c$. The first term describes the process where the electrons do not overlap in the dot, while the term $\propto e^{ik_+\xi_>}e^{ik_0\xi_<}$ deals with the case where both electrons occupy the dot simultaneously during scattering. For electrons in a spin-triplet state with anti-symmetric orbital wave function $\Psi^{\rm in}(y_1,y_2)$, this term vanishes and no interaction effects survive, a consequence of the Pauli principle.

Let us show that the Coulomb interaction in the dot leads to an orbital entanglement of the two particles (for interaction-induced spin entanglement in a quantum dot, see Ref. [30]). Here, we concentrate on the component of the wave function where two electrons are transmitted to the right and estimate its degree of entanglement, which is entirely due to the interaction in the dot. We analyze the situation where the length of the incoming wave packet is small with respect to ℓ. Then the normalized wave function on the right has the universal form:

$$\Psi_{\rm RR}(\xi_1,\xi_2)=(2/\ell)\,e^{ik_+\xi_>}e^{ik_0\xi_<}\,e^{(\xi_1+\xi_2)/\ell},\qquad(12)$$

where $\xi_{1,2}<0$. Eq. (12) describes a two-electron state with different momenta k_+ and $k_0<k_+$, as has to be expected since the first electron escaping carries an energy shifted up by the Coulomb interaction. The state (12) can be rewritten in a form

$$\Psi_{\rm RR}=(2/\ell)e^{i(k_0+\frac{k_c}{2})(\xi_1+\xi_2)}\,e^{i\frac{k_c}{2}|\xi_1-\xi_2|}e^{(\xi_1+\xi_2)/\ell},\quad(13)$$

reminding about the original Einstein-Podolsky-Rosen state [11]: $\Psi_{EPR}(x_1,x_2)=\delta(x_1-x_2+x_0)$ describing the orbitally entangled state of two particles with the fixed relative position x_0 but unknown center of mass coordinate (note that this EPR state yet has to be properly normalized). To quantify its entanglement, one may calculate the von Neumann entropy E of the reduced density matrix $\rho(x,x')=\int dx_2\,\Psi_{\rm RR}(x,x_2)\Psi^*_{\rm RR}(x',x_2)$. Instead, we determine the purity $\Pi(\rho)={\rm tr}\,\rho^2$, which is unity only for separable states and provides the lower limit $E>1-\Pi$. With $A\equiv ik_c\ell/(2-ik_c\ell)$, we find the density matrix

$$\rho(\xi,\xi')=(2/\ell)\,\theta(-\xi)\theta(-\xi')e^{(\xi+\xi')/\ell}e^{ik_0(\xi-\xi')}$$
$$\times\big[1+A\,\theta(\xi-\xi')(e^{2\xi/\ell}-e^{ik_c(\xi-\xi')}e^{2\xi'/\ell})$$
$$+A^*\theta(\xi'-\xi)(e^{2\xi'/\ell}-e^{ik_c(\xi-\xi')}e^{2\xi/\ell})\big],\qquad(14)$$

that results into a purity $\Pi=[1+2/(1+(k_c\ell/4)^2)]/3$. We conclude that at finite U_c the state (13) is entangled and the degree of entanglement saturates as the Coulomb interaction becomes larger than the resonance width, $k_c\ell=U_c/\Gamma\gg1$, i.e., when the energies of the escaped particles become distinguishable. In this case one could find $\Pi=\frac{1}{3}$ and ${\rm tr}\,\rho^3=\frac{2}{15}$ and the degree of entanglement may be estimated more precisely using an expansion $E=-{\rm tr}\{\rho\log_2\rho\}=\sum_{n=1}\frac{1}{n}{\rm tr}\{\rho(1-\rho)^n\}/\ln 2$ which gives $E>1.3$.

ENTANGLEMENT OF NONINTERACTING IDENTICAL PARTICLES

In the present section we closely follow our previous work [15]. We discuss a scheme generating pulsed spin-entangled electron pairs in a normal-metal mesoscopic structure arranged in a fork geometry, see Fig. 1. In this device, spin-entangled electron pairs are generated via the injection of spin-singlet pairs into the source lead from the reservoir. This entanglement is made accessible by splitting the pair into the two leads 'u' and 'd' and subsequent projection (through the Bell measurement) to that part of the wave function describing separated electrons travelling in different leads [31]. Rather then quantum pumping with a cyclic potential as in Refs. [32, 33], our proposal makes use of definite voltage pulses generating spin-entangled electron pairs. Below we discuss a scheme where voltage pulses of specific form accumulating one unit of flux $\Phi_0 = -c\int dt\, V(t)$ and applied to the source lead 's' generate pairs of spin-entangled electrons which then are distributed between the two outgoing leads of the fork, the upper and lower arms denoted as 'u' and 'd'. These spin-entangled electron states are subsequently analyzed in a Bell experiment [7] involving the measurement of cross-correlations [34] between the number of electrons transmitted through the corresponding spin filters in the two arms of the fork, see Fig. 1. Using time resolved correlators, we are in a position to analyze arbitrary forms of voltage pulses and determine the resulting degree of violation in the Bell setup. We find that Lorentzian shaped pulses generate spin-entangled pairs with 50 % probability, corresponding in efficiency to the optimal performance of one entangled pair per two cycles as found by Beenakker *et al.* [33]. The reduction in efficiency to 50 % is due to the competing processes where the spin-entangled pair generated by the voltage pulse propagates into only one of the two arms. In order to make use of this structure as a deterministic entangler, the Bell measurement setup has to be replaced through a corresponding projection device (post-) selecting that part of the wave function with the two electrons distributed between the two arms; alternatively, this post-selection may be part of the application device itself, as is the case in the Bell inequality measurement.

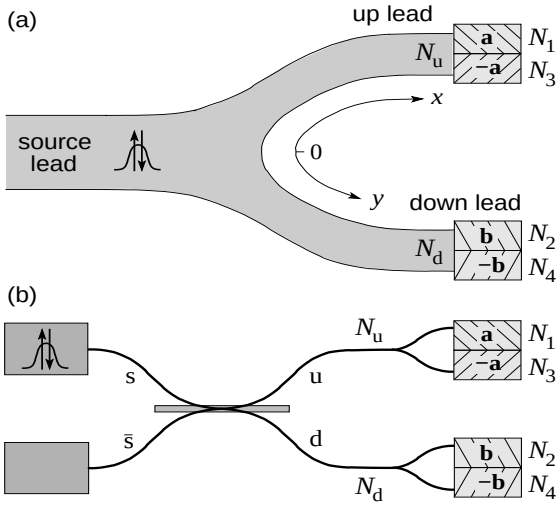

FIGURE 1.

Bell Inequality with Number Correlators

The Bell inequality [13] is based on the Lemma saying that, given a set of real numbers x, $\bar{x}$, y, $\bar{y}$, X, Y with $|x/X|$, $|\bar{x}/X|$, $|y/Y|$, and $|\bar{y}/Y|$ restricted to the interval $[0,1]$, the inequality $|xy - x\bar{y} + \bar{x}y + \bar{x}\bar{y}| \leq 2|XY|$ holds true. We define the operator of electric charge $\hat{N}_i(t_{\rm ac})$ transmitted through the i-th spin detector during the time interval $[0,t_{\rm ac}]$, where $t_{\rm ac} > 0$ is the accumulation time. The charge operator $\hat{N}_i(t_{\rm ac})$ can be expressed via the electric current $\hat{I}_i(t)$ flowing through the i-th detector, $\hat{N}_i(t_{\rm ac}) = \int_0^{t_{\rm ac}} dt'\, \hat{I}_i(t')$. In the Bell test experiment, see Fig. 1, one measures the number of transmitted electrons with a given spin polarization, N_i, $i = 1,\ldots,4$, and defines the quantities $x = N_1 - N_3$, $y = N_2 - N_4$, $X = N_1 + N_3$, and $Y = N_2 + N_4$ for fixed orientations $\mathbf{a}$ and $\mathbf{b}$ of the polarizers (and similar for $\bar{x}$ and $\bar{y}$ for the orientations $\bar{\mathbf{a}}$ and $\bar{\mathbf{b}}$), see Ref. [34]. Our Bell setup measures the correlations $\mathscr{K}_{ij}(\mathbf{a},\mathbf{b}) = \langle \hat{N}_i(t_{\rm ac})\hat{N}_j(t_{\rm ac})\rangle$ between the number of transmitted electrons N_i, $i = 1,3$, in the lead 'u' with spin polarization along $\pm\mathbf{a}$ and their partners N_j, $j = 2,4$, in lead 'd' with spin polarization along $\pm\mathbf{b}$. Using the above definitions for x, y, X, and Y, we obtain the normalized particle-number difference correlator,

$$E(\mathbf{a},\mathbf{b}) \;=\; \frac{\langle[\hat{N}_1 - \hat{N}_3][\hat{N}_2 - \hat{N}_4]\rangle}{\langle[\hat{N}_1 + \hat{N}_3][\hat{N}_2 + \hat{N}_4]\rangle}, \qquad (15)$$

and evaluating the correlators for the four different combinations of directions $\mathbf{a}$, $\bar{\mathbf{a}}$ and $\mathbf{b}$, $\bar{\mathbf{b}}$, we arrive at the Bell inequality

$$E_{\rm BI} = |E(\mathbf{a},\mathbf{b}) - E(\mathbf{a},\bar{\mathbf{b}}) + E(\bar{\mathbf{a}},\mathbf{b}) + E(\bar{\mathbf{a}},\bar{\mathbf{b}})| \leq 2. \quad (16)$$

We proceed further by extracting in $\mathscr{K}_{ij}$ the irreducible particle number correlators $K_{ij}(t_{\rm ac}) = \langle \delta\hat{N}_i(t_{\rm ac})\delta\hat{N}_j(t_{\rm ac})\rangle$ and rewrite $E(\mathbf{a},\mathbf{b})$ in the form

$$E(\mathbf{a},\mathbf{b}) = \frac{K_{12} - K_{14} - K_{32} + K_{34} + \Lambda_-}{K_{12} + K_{14} + K_{32} + K_{34} + \Lambda_+}, \qquad (17)$$

where we have defined $\Lambda_\pm = [\langle\hat{N}_1\rangle \pm \langle\hat{N}_3\rangle][\langle\hat{N}_2\rangle \pm \langle\hat{N}_4\rangle]$ and K_{ij} may be rewritten in terms of irreducible current correlators $C_{ij}(\mathbf{a},\mathbf{b};t_1,t_2) = \langle\delta\hat{I}_i(t_1)\delta\hat{I}_j(t_2)\rangle$ with

$\delta\hat{I}_i(t) = \hat{I}_i(t) - \langle\hat{I}_i(t)\rangle$,

$$K_{ij}(t_{\rm ac}) \quad = \quad \int_0^{t_{\rm ac}} dt_1 dt_2\, C_{ij}(\mathbf{a},\mathbf{b};t_1,t_2).$$

The average currents are related via $\langle\hat{I}_1(t)\rangle = \langle\hat{I}_3(t)\rangle = \langle\hat{I}_{\rm u}(t)\rangle/2$ and $\langle\hat{I}_2(t)\rangle = \langle\hat{I}_4(t)\rangle = \langle\hat{I}_{\rm d}(t)\rangle/2$ and thus $\Lambda_- = 0$, $\Lambda_+ = \langle\hat{N}_{\rm u}\rangle\langle\hat{N}_{\rm d}\rangle$. The irreducible current-current correlator factorizes into a product of spin and orbital parts, $C_{ij}(\mathbf{a},\mathbf{b};t_1,t_2) = |\langle\mathbf{a}_i|\mathbf{b}_j\rangle|^2 C_{\rm ud}(t_1,t_2)$ with $\mathbf{a}_{1,3} = \pm\mathbf{a}$ and $\mathbf{b}_{2,4} = \pm\mathbf{b}$. The spin projections involve the angle $\theta_{\mathbf{ab}}$ between the directions $\mathbf{a}$ and $\mathbf{b}$ of the polarizers, $\langle\pm\mathbf{a}|\pm\mathbf{b}\rangle = \cos^2(\theta_{\mathbf{ab}}/2)$ and $\langle\pm\mathbf{a}|\mp\mathbf{b}\rangle = \sin^2(\theta_{\mathbf{ab}}/2)$, and the Bell inequality assumes the form

$$\left|\frac{K_{\rm ud}[\cos\theta_{\mathbf{ab}} - \cos\theta_{\mathbf{a\bar{b}}} + \cos\theta_{\mathbf{\bar{a}b}} + \cos\theta_{\mathbf{\bar{a}\bar{b}}}]}{2K_{\rm ud} + \langle\hat{N}_{\rm u}\rangle\langle\hat{N}_{\rm d}\rangle}\right| \leq 1, \quad (18)$$

where $K_{\rm ud}(t_{\rm ac}) = \int_0^{t_{\rm ac}} dt_1 dt_2\, C_{\rm ud}(t_1,t_2)$ is the (irreducible) number cross-correlator between the upper and lower leads of the fork. The maximal violation of the Bell inequality is attained for the standard orientations of the detector polarizations $\theta_{\mathbf{ab}} = \theta_{\mathbf{\bar{a}b}} = \theta_{\mathbf{\bar{a}\bar{b}}} = \pi/4$, $\theta_{\mathbf{a\bar{b}}} = 3\pi/4$; the Bell inequality (18) then reduces to

$$E_{\rm BI} = \left|\frac{2K_{\rm ud}}{2K_{\rm ud} + \langle\hat{N}_{\rm u}\rangle\langle\hat{N}_{\rm d}\rangle}\right| \leq \frac{1}{\sqrt{2}}. \quad (19)$$

Number Correlators for a Single Pulse

The orbital part $C_{\rm ud}(t_1,t_2)$ of the current cross-correlator between the upper and lower leads can be calculated within the standard scattering theory of noise [2]. We assume that the time dependent voltage drop $V(t)$ at the splitter can be treated adiabatically (i.e., the voltage changes slowly during the electron scattering time). Such approach have first been used in the calculation of the spectral noise power in an *ac*-driven system [35] and its validity has been confirmed in several experiments [36].

In the limit of linear dispersion the irreducible current cross-correlator $C_{\rm ud}(t_1,t_2) = \langle\delta\hat{I}_{\rm u}(x,t_1)\delta\hat{I}_{\rm d}(y,t_2)\rangle$ measured at the positions x and y in the leads 'u' and 'd' can be splitted into two terms, one due to equilibrium fluctuations, $C^{\rm eq}_{\rm ud}(t_1-t_2) = \int(d\omega/2\pi)\,S^{\rm eq}(\omega)e^{i\omega(t_1-t_2)}$ with

$$S^{\rm eq}(\omega) = -\frac{2e^2}{h}\,T_{\rm ud}\cos(\omega\tau^+)\,\frac{\hbar\omega}{1-e^{\hbar\omega/\theta}}, \quad (20)$$

and a second term describing the excess correlations at finite voltage,

$$C^{\rm ex}_{\rm ud}(t_1,t_2) = -\frac{4e^2}{h^2}T_{\rm u}T_{\rm d}\sin^2\frac{\phi(\xi_1)-\phi(\xi_2)}{2}\,\alpha(\tau-\tau^-,\theta), \quad (21)$$

with $\alpha(\tau,\theta) = \pi^2\theta^2/\sinh^2[\pi\theta\tau/\hbar]$ (θ is the temperature of electronic reservoirs), $\tau = t_1 - t_2$, $\tau^\pm = (x\pm y)/v_{\rm F}$, $\xi_1 = t_1 - x/v_{\rm F}$, and $\xi_2 = t_2 - y/v_{\rm F}$. The coefficients $T_{\rm u}$, $T_{\rm d}$, and $T_{\rm ud}$ denote the transmission probabilities from the source to the 'up', 'down' leads, and between the 'down' and the 'up' leads.

The equilibrium correlator $C^{\rm eq}_{\rm ud}$ describes the correlations of the electrons in the Fermi sea propagating ballistically from lead 'u' to lead 'd' (or vice versa) with the retardation $\tau^+ = (x_1+x_2)/v_{\rm F}$. The corresponding equilibrium part of the particle-number cross-correlator, $K^{\rm eq}_{\rm ud} = \int_0^{t_{\rm ac}} dt_1 dt_2\, C^{\rm eq}_{\rm ud}(t_1-t_2)$ then takes the form

$$K^{\rm eq}_{\rm ud} \approx \frac{e^2}{\pi^2}T_{\rm ud}\ln\frac{t_{\rm ac}}{\tau}, \quad \tau = \max\{\hbar/\varepsilon_{\rm F},\tau^+\}, \quad (22)$$

where we have assumed the zero temperature limit and an accumulation time $t_{\rm ac} \gg \tau$. The logarithmic divergence in $t_{\rm ac}$ reduces the violation of the Bell inequality Eq. (19) at large accumulation times and one has to suppress the equilibrium correlations between the upper and the lower leads in the setup. This can be achieved via a reduction in the transmission probability $T_{\rm ud}$, however, in the fork geometry of Fig. 1(a) the probability $T_{\rm ud}$ cannot be made to vanish. Alternatively, one may chose a setup with a reflectionless four-terminal beam splitter as sketched in Fig. 1(b) with no exchange amplitude between the upper and lower outgoing leads and thus $K^{\rm eq}_{\rm ud} = 0$.

Next, we concentrate on the excess part $K^{\rm ex}_{\rm ud}$ of the particle-number cross-correlator $\langle\hat{N}_{\rm u}(t_{\rm ac})\hat{N}_{\rm d}(t_{\rm ac})\rangle$. Note that the excess fluctuations are the same for both setups Fig. 1(a) and (b) and we can carry out all the calculations for the fork geometry. We consider a sharp voltage pulse applied at time t_0, $0 < t_0 < t_{\rm ac}$, with short duration δt. The total accumulated phase $\phi(t)$ then exhibits a step-like time dependence with the step height $\Delta\phi = \phi(t_0+\delta t/2) - \phi(t_0-\delta t/2) = -2\pi\Phi/\Phi_0$, where we have introduced the Faraday flux $\Phi = -c\int V(t)dt$ and $\Phi_0 = hc/e$ is the flux quantum. The excess part of the particle-number cross-correlator $K_{\rm ud}$ then takes the form (we consider again the zero temperature limit)

$$K^{\rm ex}_{\rm ud} = -\frac{e^2}{\pi^2}T_{\rm u}T_{\rm d}\int_0^{t_{\rm ac}} dt_1 dt_2\,\frac{\sin^2[(\phi(t_1)-\phi(t_2))/2]}{(t_1-t_2)^2}. \quad (23)$$

For a sharp pulse with $\delta t \ll t_0, t_{\rm ac}$ we can identify two distinct contributions arising from the integration domains $|t_1-t_2| \ll \delta t$ and $|t_1-t_2| \gg \delta t$, cf. Refs. [5, 37]; we denote them with $K^<$ and $K^>$. Introducing the average and relative time coordinates $t = (t_1+t_2)/2$ and $\tau = t_1 - t_2$ and expanding the phase difference $\phi(t_1) - \phi(t_2) = \phi(t+\tau/2) - \phi(t-\tau/2) \approx \dot{\phi}(t)\tau$, the first contribution $K^<$ reads

$$K^< \approx -\frac{e^2}{2\pi}T_{\rm u}T_{\rm d}\int_0^{t_{\rm ac}} dt\,|\dot{\phi}(t)|. \quad (24)$$

Assuming $\phi(t)$ is a monotonic function of t Eq. (24) can be rewritten in terms of the Faraday flux Φ,

$$K^{<} = -e^2 T_{\rm u} T_{\rm d} \frac{|\Phi|}{\Phi_0}. \tag{25}$$

Assuming the Lorenzian form of the voltage pulse carrying for integer $n = |\Phi|/\Phi_0$ exactly n (spinless) electrons [23], the particle-number cross-correlator $K^{\rm ex}_{\rm ud}$ describes the correlations arising from the n additional particles pushed through the fork by the voltage pulse $V(t)$.

The second contribution $K^{>}$ to $K^{\rm ex}_{\rm ud}$ originates from the time domains $0 < t_{1(2)} < t_0 - \delta t/2$ and $t_0 + \delta t/2 < t_{2(1)} < t_{\rm ac}$, where $|\phi(t_1) - \phi(t_2)| = 2\pi\Phi/\Phi_0$, hence

$$K^{>} \approx -\frac{2e^2}{\pi^2} T_{\rm u} T_{\rm d} \sin^2 \frac{\pi\Phi}{\Phi_0} \ln \frac{t_{\rm m}}{\delta t}; \tag{26}$$

here, we have kept the most divergent term in the measurement time $t_{\rm m} = t_{\rm ac} - t_0$, the time during which the pulse manifests itself in the detector. The above expression describes the response of the electron gas to the sudden perturbation $V(t)$; the logarithmic divergence in the measurement time $t_{\rm m}$ can be interpreted [37] along the lines of the orthogonality catastrophe [38], with the isolated perturbation in space, the impurity, replaced by the sudden perturbation in time. The periodicity of the response in the Faraday flux Φ is due to the discrete nature of electron transport as expressed through the binomial character of the distribution function of transmitted particles [5, 37]. Remarkably, the above logarithmically divergent contribution to $K^{\rm ex}_{\rm ud}$ vanishes for voltage pulses carrying an integer number of electrons.

Finally, the average number of transmitted (spinless) particles are given by $\langle \hat{N}_{\rm u(d)}(t_{\rm ac})\rangle = \int_0^{t_{\rm ac}} dt\, \langle \hat{I}_{\rm u(d)}(x,t)\rangle$, where within the scattering matrix approach,

$$\langle \hat{I}_{\rm u(d)}(x,t)\rangle = \frac{e}{h} T_{\rm u(d)}\, eV(t - x/v_{\rm F}), \tag{27}$$

and hence,

$$\langle \hat{N}_{\rm u(d)}(t_{\rm ac})\rangle = eT_{\rm u(d)} \frac{\Phi}{\Phi_0}. \tag{28}$$

Pulse with integer flux

Substituting the above expressions for the particle-number cross-correlators and for the average number of transmitted particles into (19) we arrive at the following general result for the Bell inequality

$$E_{\rm BI} = \left| \frac{n + (2/\pi^2)\sin^2(\pi n)\ln(t_{\rm m}/\delta t)}{2n^2 - n - (2/\pi^2)\sin^2(\pi n)\ln(t_{\rm m}/\delta t)} \right|. \tag{29}$$

For Lorenzian voltage pulse with integer n all logarithmic terms vanish, leaving us with the Bell inequality

$$E_{\rm BI} = \left| \frac{1}{2n-1} \right| \leq \frac{1}{\sqrt{2}}, \tag{30}$$

which we find maximally violated for $n = 1$ and never violated for larger integers $n > 1$ — any additional particle accumulated in the detector spoils the violation of the Bell inequality. Furthermore, this violation is independent of the transparencies $T_{\rm u}$, $T_{\rm d}$ and hence universal; moreover, the Bell inequality (30) does not depend on duration of the voltage pulse but involves only the number of electrons n carried by it.

The Lorenzian voltage pulse with $n = 1$ pushes two electrons with opposite spin polarization towards the beam splitter. Such a pair appears in a singlet state and can be described by the wave function $\Psi^{12}_{\rm in} = \phi^1_{\rm s}\phi^2_{\rm s}\chi^{12}_{\rm sg}$ with the spin-singlet state $\chi^{12}_{\rm sg} = [\chi^1_\uparrow\chi^2_\downarrow - \chi^1_\downarrow\chi^2_\uparrow]/\sqrt{2}$; $\phi_{\rm s}$ is the orbital part of the wave function describing a particle in the source lead 's' and the upper indices 1 and 2 denote the particle number. This local spin-singlet pair is scattered at the splitter and the wave function $\Psi^{12}_{\rm in}$ transforms to $\Psi^{12}_{\rm scat} = t^2_{\rm su}\phi^1_{\rm u}\phi^2_{\rm u}\chi^{12}_{\rm sg} + t^2_{\rm sd}\phi^1_{\rm d}\phi^2_{\rm d}\chi^{12}_{\rm sg} + t_{\rm su}t_{\rm sd}[\phi^1_{\rm u}\phi^2_{\rm d} + \phi^1_{\rm d}\phi^2_{\rm u}]\chi^{12}_{\rm sg}$, where the last term describes two particles in a singlet state shared between the upper and lower leads of the fork. The Bell inequality test is only sensitive to pairs of particles propagating in different arms, implying a projection of the scattered wave function $\Psi^{12}_{\rm scat}$ onto the spin-entangled component. Thus the origin of the entanglement is found in the post-selection during the cross-correlation measurement effectuated in the Bell inequality test [31]. From an experimental point of view it may be difficult to produce voltage pulses driving exactly one (spinless) particle $n = 1$. However, as follows from the full expression Eq. (29), for a sufficiently small deviation $|\delta n| = |n - 1| \ll 1$ the logarithmic terms are small in the parameter $(\delta n)^2$ and thus can be neglected, provided the measurement time t_m satisfies the condition $(\delta n)^2 \ln(t_{\rm m}/\delta t) \ll 1$. The same argument applies to the case of pumping with an alternating signal [32, 33]. Even if the two-particle Bell inequality may be violated when the average injected current vanishes still it does not guarantee the creation of entangled electron pairs, see Ref. [15] for details.

CONCLUSION

We have studied two different setups where entanglement of an electron pair is produced either by involving interaction between electrons or by projective measurement or post-selection. In contrast to the first method the entanglement due to post-selection appears only for the indistinguishable particles. In the interacting case a singlet electron pair is scattered on a single level quantum dot with Coulomb interaction. The resulting two-particle scattering state becomes orbitally entangled for $U_c \gg \Gamma$ (U_c - Coulomb repulsion energy, Γ is the resonance width). In order to quantify the produced entan-

glement we have estimated the von Neumann entropy of the single-electron density matrix ρ. Although the density matrix in principle can be measured directly we have not described the realistic scheme for such measurement. Calculating the purity $\Pi = \mathrm{tr}\{\rho^2\}$ and $\mathrm{tr}\{\rho^3\}$ the degree of entanglement of the scattered wave function component where both electrons are transmitted through the dot can be estimated as $E > 1.3$ of the spin-singlet entangled state.

In the setup involving a post-selection the following steps lead to the appearance of the spin-entangled state [31]: i) the Fermi statistics allows one to extract a electron spin-singlet state with the same orbit out of the Fermi sea; ii) the beam splitter directs the mixed product state into the two leads thus organizing their spatial separation, iii) a coincidence measurement projects the mixed product state onto its (spin-)entangled component describing the electron pair split between the two leads. In this situation we have suggested a realistic scheme for the Bell test involving the measurement of particle number cross-correlators. It is shown that the corresponding Bell inequality is maximally violated indicating the maximally entangled spin state of the electron pair.

Both these schemes rely on the existence of the electron source which allows one to sent a finite number of electrons in a pure quantum state, see Ref. [24] for theoretical proposal and Ref. [25] for recent experimental advances in this direction. Alternatively [23] one may apply to a electronic reservoir a voltage pulse of the Lorenzian form with integer Faraday flux $\Phi = -c\int dtV(t) = n\Phi_0$ extracting exactly n electrons (per spin component) not entangled with the Fermi sea.

ACKNOWLEDGMENTS

We acknowledge the financial support from the Swiss National Foundation (through the program MaNEP and the CTS-ETHZ), the Russian Foundation for Basic Research (08-02-00767a), and the program 'Quantum Macrophysics' of the RAS.

REFERENCES

1. M. Born, Z. Physik **37**, 863 (1926).
2. G.B. Lesovik, JETP Lett. **49**, 592 (1989); Th. Martin and R. Landauer, Phys. Rev. B **45**, 1742 (1992); Ya.M. Blanter and M. Büttiker, Phys. Rep. **336**, 1 (2000).
3. M. Reznikov *et al.*, Phys. Rev. Lett. **75**, 3340 (1995); A. Kumar *et al.*, Phys. Rev. Lett. **76**, 2778 (1996).
4. L. Saminadayar *et al.*, Phys. Rev. Lett. **79**, 2526 (1997); R. de-Picciotto *et al.*, Nature **389**, 162 (1997).
5. L.S. Levitov and G.B. Lesovik, JETP Lett. **58**, 230 (1993); L.S. Levitov, H. Lee, and G.B. Lesovik, J. Math. Phys. **37**, 4845 (1996).
6. S. Gustavsson *et al.*, Phys. Rev. Lett. **96**, 076605 (2006).
7. J.S. Bell, Physics **1**,195 (1965).
8. L. D. Landau, Z. Physik **45**, 430 (1927).
9. J. v on Neumann, Gottinger Nachr., 245 (1927).
10. L. D. Landau and E. M. Lifshitz, *Qunatum Mechanics* (Pergamon Press, London, 1958), Vol. 3 Sec. 14.
11. A. Einstein, B. Podolsky, and N. Rosen, Phys. Rev. **47**, 777 (1935).
12. E. Schroedinger, Naturwiss. **23**, 807 (1935).
13. J.F. Clauser and M.A. Horne, Phys. Rev. D **10**, 526 (1974).
14. G. Lesovik, T. Martin, and G. Blatter, Eur. Phys. J. B **24**, 287 (2001); P. Recher, E.V. Sukhorukov, and D. Loss, Phys. Rev. B **63**, 165314 (2001); C.W.J. Beenakker, C. Emary, M. Kindermann, and J.L. van Velsen, Phys. Rev. Lett. **91**, 147901 (2003).
15. A.V. Lebedev, G.B. Lesovik, and G. Blatter, Phys. Rev. B **72**, 245314 (2005).
16. C. W. J. Beenakker, in *Quantum Computers, Algorithms and Chaos*, Proceedings of the International School of Physics "Enrico Fermi" Varenna, 2005 (IOS, Amsterdam, 2006), Vol. 162.
17. A. Aspect, Nature **398**, 189 (1999) and reference therein.
18. L. Amico, R. Fazio, A. Osterloh, and V. Vedral, Rev. Mod. Phys. **80**, 517 (2008).
19. A.V. Lebedev, G.B. Lesovik, and G. Blatter, Phys. Rev. Lett. **100**, 226805 (2008).
20. S. Bose and D. Home, Phys. Rev. Lett. **88**, 050401 (2002).
21. J.A. Wheeler, Phys. Rev. **52**, 1107 (1937); W. Heisenberg, Z. Physik **120**, 513 and 673 (1943).
22. R. Landauer, IBM J. Res. Dev. **1**, 223 (1957); R. Landauer, Philosoph. Mag. **21**, 863 (1970).
23. D.A. Ivanov and L.S. Levitov, JETP Lett. **58**, 461 (1993); J. Keeling, I. Klich, and L.S. Levitov, Phys. Rev. Lett. **97**, 116403 (2006); F. Hassler, G.B. Lesovik, and G. Blatter, Phys. Rev. Lett. **99**, 076804 (2007).
24. J. Keeling, A.V. Shytov, L.S. Levitov, arXiv:0804.4281.
25. G. Feve *et al.*, Science **316**, 1169 (2007); A. Mahé, *et al.*, arXiv:0809.2727.
26. P.W. Anderson, Phys. Rev. **124**, 41 (1961).
27. D.T. McClure *et al.*, Phys. Rev. Lett. **98**, 056801 (2007).
28. M.C. Goorden and M. Büttiker, Phys. Rev. Lett. **99**, 146801 (2007).
29. L.I. Glazman and M.E. Raikh, JETP Lett. **47**, 452 (1988).
30. W.D. Oliver, F. Yamaguchi, and Y. Yamamoto, Phys. Rev. Lett. **88**, 037901 (2002).
31. A.V. Lebedev, G. Blatter, C.W.J. Beenakker, and G.B. Lesovik, Phys. Rev. B **69**, 235312 (2004).
32. P. Samuelsson and M. Büttiker, Phys. Rev. B **71**, 245317 (2005).
33. C.W.J. Beenakker, M. Titov, and B. Trauzettel, New J. Phys. **7**, 186 (2005).
34. N.M. Chtchelkatchev, G. Blatter, G.B. Lesovik, and T. Martin, Phys. Rev. B **66**, 161320(R) (2002).
35. L.S. Levitov and G.B. Lesovik, Phys. Rev. Lett. **72**, 538 (1994);
36. A.A. Kozhevnikov, R.J. Schoelkopf, and D.E. Prober, Phys. Rev. Lett. **84**, 3398 (2000); L.-H. Reydellet, P. Roche, D.C. Glattli, B. Etienne, and Y. Jin, Phys. Rev. Lett. **90**, 176803 (2003).
37. H. Lee and L.S. Levitov, cond-mat/9312013.
38. P.W. Anderson, Phys. Rev. Lett. **18**, 1049 (1967).